Journal for ImmunoTherapy of Cancer

Tempered signal strength via low-dose MEK inhibition optimizes therapeutic performance of engineered T cells

Franziska Füchsl ,[1,2] Antonia Schwanzer,[1,2] Melanie Faber,[1,2] Leonie Rieger,[1,2] Gabriela Zuleger ,[1,2] Priska Auf der Maur ,[1,2] Emmanuel Cruz,[1,2] Sarah Braun ,[3] Rupert Öllinger,[4] Dirk H Busch,[3,5] Florian Bassermann,[1,2,6,7] Angela M Krackhardt [1,2,7]

To cite: Füchsl F, Schwanzer A, Faber M, *et al*. Tempered signal strength via low-dose MEK inhibition optimizes therapeutic performance of engineered T cells. *Journal for ImmunoTherapy of Cancer* 2025;**13**:e012800. doi:10.1136/jitc-2025-012800

► Additional supplemental material is published online only. To view, please visit the journal online (https://doi.org/10.1136/jitc-2025-012800).

Parts of the data in this study were previously presented at the 5th International Conference on Lymphocyte Engineering (ICLE), held in Munich.

Accepted 14 October 2025

Check for updates

© Author(s) (or their employer(s)) 2025. Re-use permitted under CC BY-NC. No commercial re-use. See rights and permissions. Published by BMJ Group.

For numbered affiliations see end of article.

Correspondence to
Franziska Füchsl;
franziska.fuechsl@tum.de

ABSTRACT

Background Optimizing T cell activation strength is emerging as a critical factor in improving adoptive cellular therapy (ACT). We previously reported that neoantigen-specific T cell receptor (TCR) clonotypes from a patient with metastatic melanoma exhibited enhanced resilience to repeated stimulation when initially activated at moderate levels.

Methods Building on these observations, we applied transient, low-dose MEK inhibition (MEKi) to fine-tune T cell signal strength during early activation. We evaluated this combinatorial strategy in vitro using co-cultures of CD8+ T cells engineered with patient-derived neoantigen-specific TCRs, alongside chimeric antigen receptor-T cells, bispecific T cell engagers, and non-engineered tumor-infiltrating lymphocytes (TILs). In vivo efficacy was evaluated in a xenograft model with intravenous TCR-T cell transfer and systemic low-dose MEKi.

Results MEKi co-treatment induced a more tempered activation profile that enhanced T cell proliferation, fitness, and persistence under strong stimulation. These effects were consistent across various in vitro and in vivo models for engineered T cells as well as primary melanoma-derived TILs. MEKi dampened the pro-inflammatory T cell activation profile, most notably diminishing tumor necrosis factor (TNF) secretion, mechanistically driven by coordinated and selective disruption of the key transcriptional regulators nuclear factor kappa-light-chain-enhancer of activated B cells (NFκB) and nuclear factor of activated T cells (NFAT) while partly preserving activator protein 1 (AP-1) activity.

Conclusion These findings highlight moderate activation as a critical determinant of engineered T cell long-term performance. Low-dose MEKi offers a therapeutic tool for fine-tuning T cell activation and enhancing ACT efficacy.

WHAT IS ALREADY KNOWN ON THIS TOPIC

⇒ Moderate T cell activation enhances the durability and function of neoantigen-specific T cell receptor (TCR)-based T cells during repeated tumor stimulation.

WHAT THIS STUDY ADDS

⇒ Transient, low-dose MEK inhibition (MEKi) selectively tempers activation strength, promoting T cell persistence and improving therapeutic performance across ACT platforms.

HOW THIS STUDY MIGHT AFFECT RESEARCH, PRACTICE OR POLICY

⇒ MEKi-based signal tuning emerges as a clinically accessible strategy to optimize T cell activation and enhance outcomes in adoptive cell therapy.

BACKGROUND

Adoptive cellular therapies (ACT) employing genetically engineered T cells have become increasingly important for the treatment of refractory cancer patients. Alongside established chimeric antigen receptor (CAR)-T cell therapies for B cell malignancies,[1] recently, the first T cell receptor (TCR)-based T cell therapies were approved for clinical use.[2 3] Further clinical studies of TCR-T cells promise potential for broader implementation in therapeutic regimens and earlier lines of therapy.[4–6] TCR-based therapies target numerous groups of antigens spanning the entire tumor cell peptidome presented on major histocompatibility complexes (MHC), including non-mutated tumor-associated self-antigens[7] or mutated neoepitopes.[5 6 8–10] However, repertoires of tumor-specific TCR-clonotypes[8 11 12] raise the question about the optimal 'goldilocks' signal strength of TCRs for use in ACT. While previous therapeutic approaches prioritized receptors with high functional avidity,[8 13–15] we recently reported an inverse relationship of TCR-T cell activation levels and resilience on rechallenge. TCR-transgenic (tg) T cells with more moderate initial activation and lower functional avidity showed improved T cell persistence upon repeated tumor encounter.[11] Similar avidity-dependent patterns were observed in different murine models, suggesting higher levels of exhaustion and ineffective antitumor

Journal for ImmunoTherapy of Cancer: first published as 10.1136/jitc-2025-012800 on 1 December 2025. Downloaded from https://jitc.bmj.com on 12 February 2026 by guest. Protected by copyright, including for uses related to text and data mining, AI training, and similar technologies.

activity in high-avidity TCR-clonotypes.[16 17] Leveraging insights from these TCR repertoires, we hypothesize that transient, low-level inhibition of TCR signaling during early activation can enhance the performance of strongly activated, TCR-engineered T cells.

To achieve transient inhibition rather than permanent genetic modification, we employed small-molecule kinase inhibitors. Previous data showed that application of several kinase inhibitors during ex vivo expansion of CAR-T cells prevented tonic signaling and promoted memory phenotypes.[18–20] Moreover, the combination of CAR-T cells with the Src tyrosine kinase inhibitor dasatinib (DASA) as a pharmacological off-switch for steering CAR-T cell activity could prevent cytokine release syndrome (CRS) and partly restore exhaustion.[20–22] However, while DASA broadly targets multiple tyrosine kinases,[23] we sought a more selective kinase inhibitor that would partially attenuate, rather than fully suppress, TCR signaling. Among the core pathways downstream TCR engagement are three major transcription factors that orchestrate T cell activation, differentiation, and function—mitogen-activated protein kinase (MAPK) via activator protein 1 (AP-1), nuclear factor kappa-light-chain-enhancer of activated B cells (NFκB), and nuclear factor of activated T cells (NFAT). The MEK inhibitor (MEKi) cobimetinib (COB), clinically first approved for combinatorial treatment with vemurafenib for $BRAF^{V600}$-mutated metastasized melanoma, allosterically targets MEK1 and, with lower potency, MEK2, both part of the MAPK pathway.[24 25] Previous combinatorial approaches of MEKi with immune checkpoint inhibitor (ICI) therapy have already highlighted the potential of MEKi to enhance CD8 T cell responses[26 27] and sustain a more memory stem cell-like phenotype upon MEKi treatment.[27] However, clinical studies evaluating this combination have so far yielded only modest therapeutic benefit.[28–30] Recently, the addition of MEKi during CAR-T cell manufacturing and tumor encounter prevented terminal differentiation driven by tonic signaling or antigen-induced activation.[31] However, comparable data for TCR-engineered T cell therapies are still lacking.

In this work, we demonstrate that MEKi decreases TCR-T cell activation levels, enhancing their resistance to overstimulation and their efficacy under conditions of strong TCR signaling, such as high tumor load. We provide evidence for increased fitness and proliferation in T cells across various in vitro, in vivo, and ex vivo experimental systems investigating engineered and non-engineered T cells. These effects are driven by MEKi-mediated modulation of the T cell inflammatory profile, most notably reflected in the near-complete abrogation of tumor necrosis factor (TNF) secretion. Mechanistically, this outcome is linked to coordinated suppression of promoter activity of NFκB and NFAT, while partially preserving AP-1 activity, which our data suggest is central to the increase in T cell persistence. Overall, low-dose MEKi co-treatment enhances TCR-T cell-mediated tumor control, supporting its use in fine-tuned combinatorial and engineering strategies to improve ACT.

METHODS

Generation of CD8+ T cells transgenic for neoantigen-specific TCRs or aCD19-CAR

Retroviral transduction

CD8+ T cells were obtained by magnetic negative selection from healthy donor-derived peripheral blood mononuclear cells (PBMCs) (EasySep Human $CD8^+$ T Cell Isolation Kit, Stemcell, catalog 17953) and activated for 48 hours with 30 U/mL human interleukin (IL)-2 and anti-CD3-anti-CD28-beads (Dynabeads human T-activator CD3/CD28, Thermo Fisher, catalog 11131D). Retroviral packaging cells RD114 were seeded to reach a confluency of 60% on the day of transfection and subsequently transfected with plasmids containing the neoantigen-specific TCR (neoTCR)-α-chain and -β-chain sequences[10 11] or CAR-T cell construct[32] (aCD19-28z-CAR or aCD19-41BBz-CAR, kindly provided by Professor Feuchtinger, Freiburg) using TransIT-293 (MirusBio, catalog MIR 2700). Transfected cells were incubated for 48 hours, supernatants were subsequently filtered and used for spin infection of activated CD8+ T cells. Transduced T cells were cultivated with IL-7 and IL-15 for 10 days as described before.[9] Transduction efficiencies were determined via flow cytometry staining with an antibody against the murine β-chain of engineered TCR-constructs in comparison with non-transduced T cell populations.

Orthotopic T cell receptor replacement via CRISPR/Cas9 knock-in

CRISPR/Cas9-mediated TCR engineering was done as described before[33 34] (see also online supplemental methods). After 5 days of cultivation, orthotopic TCR replacement (OTR)-modified cells were enriched for TCRmu+ cells on an Aria Fusion cell sorter (BD). Cells were then expanded with irradiated feeder cells in Roswell Park Memorial Institute medium supplemented with 5% human serum, 180 IU/mL IL-2, and 1 µg/mL phytohemagglutinin (PHA). Five days before experiments, no more PHA was added, and IL-2 was reduced to 50 IU/mL.

In vitro assessment of effector responses and quantitative dynamics in TCR-tg, OTR-engineered, or CAR-tg T cells on MEKi co-treatment: co-culture setup

The functional and phenotypic aspects were assessed within co-culture settings using retrovirally tg or OTR-engineered CD8+ T cells from different healthy donors and different target cells. Target cell lines (U698M, JJN3 B27) were either tg for the tandem minigene (mutated minigene (mut mg) vs wildtype minigene (wt mg)) or pulsed (2 hours at 37°C) with different concentrations of peptides $KIF2C^{P13L}$ and $SYTL4^{S363F}$ or their wildtype form. TCR-tg or OTR-engineered TCRmu+ T cells were considered effector cells for all effector-to-target (E:T) ratios unless indicated otherwise. For MEKi in most analyses, the inhibitor COB (MedChem Express, catalog

Journal for ImmunoTherapy of Cancer: first published as 10.1136/jitc-2025-012800 on 1 December 2025. Downloaded from https://jitc.bmj.com on 12 February 2026 by guest. Protected by copyright, including for uses related to text and data mining, AI training, and similar technologies.

HY-13064) was added to the co-culture from its beginning (0 hour) if not stated otherwise at concentrations indicated for each experiment. To compare different MEKi, we performed analyses comprising five different MEKi (all MedChem Express): selumetinib (SELU) (catalog HY-50706), binimetinib (BINI) (catalog HY-15202), COB, GDC-0623 (GDC) (catalog HY-15610), trametinib (catalog HY-10999). All MEKi were dissolved in dimethyl sulfoxide (DMSO) and used at concentrations indicated per experiment. For comparative analyses, DASA (Merck, catalog SML2589) was also dissolved in DMSO and used at concentrations indicated per experiment.

In vivo tumor rejection potential in a xenograft model

NOD.CG-Prkdcscid IL2rgtm1Wjl/SzJ (NSG; The Jackson Laboratory, RRID: IMSR_JAX:021885) were maintained according to the institutional guidelines and approval of local authorities (Regierung von Oberbayern; ROB-55.2-2532.Vet_02-19-125). A xenograft murine model was established as previously described.[35] Animal well-being was assessed daily, and tumor growth was monitored in vivo by external measurements with digital caliper until end point criteria as regulated in ROB-55.2-2532.Vet_02-19-125 were achieved. Mice were euthanized by isoflurane and cervical dislocation on achievement of endpoint criteria or end of experiment.

The capacity of primary tumor control was assessed as described before.[10] Briefly, male and female NSG mice at the age of 6–10 weeks were subcutaneously injected with U698M-mut mg cells (10×10^6 cells/flank). As tumors reached an area of 20 mm^2, T cells transduced with neoTCR KIF-sc1 or an irrelevant TCR (2.5D6 targeting MPO[35]) were injected intravenously. A total of 3×10^6 neoTCR-tg T cells (KIF-sc1) were administered intravenously to U698M-mut mg-tumor bearing mice. Either on the day of T cell injection (day 0) or at a later time point (day 3), tumor-bearing mice received an additional intraperitoneal injection of either COB at the indicated dose (0.25, 1, or 7.5 mg/kg of body weight (bw)) in phosphate-buffered saline (PBS) or PBS with equal amount of DMSO. Male and female animals as well as animals of different ages were distributed evenly across all treatment groups. Tumor growth kinetics were monitored daily for up to 12 weeks with blinded measurement by digital caliper until experiment endpoint criteria were reached.

Triple parameter reporter system for analysis of TCR signaling

JE6.1 Jurkat cells, transduced to express a triple-parameter reporter (TPR) platform for NFAT, NFκB, and AP-1,[36] along with CD8α and CD8β chain[37] (kindly provided by Professor Peter Steinberger, University of Vienna), were retrovirally transduced to express neoTCRs derived from the repertoire of patient Mel15.[10 11] For signaling analysis, co-cultures were set up as described before and reporter activity measured by flow cytometric analysis (enhanced green fluorescent protein: NFAT, enhanced cyan fluorescent protein: NFκB and MCherry fluorescent protein: AP-1).

Bulk RNA sequencing and data analysis

For analysis of transcriptomic differences, co-culture was set up at E:T 1:4 with KIF-sc1-tg TCR-T cells from three different donors and lymphoma cell line U698M-mut mg for 20 hours and 96 hours. At each time point, CD8+ T cells were purified by CD8-MACS (Miltenyi Biotec). CD8+ T cells were immediately snap frozen and total RNA was isolated for all co-culture conditions as well as unstimulated T cells using the RNeasy Mini Kit (Qiagen, catalog 74104) according to the manufacturer's instructions. Library preparation for bulk-sequencing of poly(A)-RNA was performed as published previously[38] and data analyzed using the DESeq2[39] (V.1.46.0) R package (see also online supplemental methods).

Statistics

Differences between conditions in vitro were assessed by ordinary one-way analysis of variance (ANOVA) and Tukey's or Dunnett's multiple comparison test. Differences between different conditions in the xenograft model were analyzed by ordinary one-way ANOVA with Tukey's correction for multiple comparisons or unpaired t-test as indicated in the figure legends. Statistical comparison of survival was performed using the Mantel-Cox test. Statistical analyses were performed with GraphPad Prism V.9.3.1 software.

RESULTS

MEKi decreases the activation level of TCR-engineered T cells following non-specific and TCR-specific activation

While clinically first approved for the antiproliferative treatment of metastasized melanoma, we investigated the effect of the MEKi COB on CD8+ T cell activation. Therefore, we stimulated CD8+ TCR tg T cells non-specifically with phorbol 12-myristate 13-acetate (PMA) and ionomycin (Iono) in vitro and, expectedly, detected a decrease of phospho-p42/44 (ERK1/2), the kinases directly downstream of MEK, on addition of MEKi (figure 1a,b). Meanwhile, COB treatment in this dose range (below 1 µM) did not affect tumor growth of different tumor cell lines (figure 1c), demonstrating that any effect on tumor cell survival after TCR engagement is mediated by the T cells themselves, rather than a direct effect of the MEKi at this concentration.

Hypothesizing that MEKi would lower TCR-tg T cell activation, we focused on a neoTCR—KIF-sc1—with a strong activation profile as previously described.[11] This neoTCR was identified in an oligoclonal TCR repertoire with identical neoepitope-MHC-specificity in a patient with metastasized melanoma by a single-cell TCR-sequencing-enforced pipeline.[11] The neoepitope recognized, $KIF2C^{P13L}$, had been identified by mass spectrometry-based neoantigen detection.[9 40] After generating TCR-tg CD8+ T cells from healthy donor PBMCs, we co-cultured KIF-sc1-tg T cells with the lymphoma cell line U698M-mut mg or multiple myeloma (MM) cell line JJN3 B27-mut mg, both tg for the neoantigen $KIF2C^{P13L}$. We stained for

Journal for ImmunoTherapy of Cancer: first published as 10.1136/jitc-2025-012800 on 1 December 2025. Downloaded from https://jitc.bmj.com on 12 February 2026 by guest. Protected by copyright, including for uses related to text and data mining, AI training, and similar technologies.

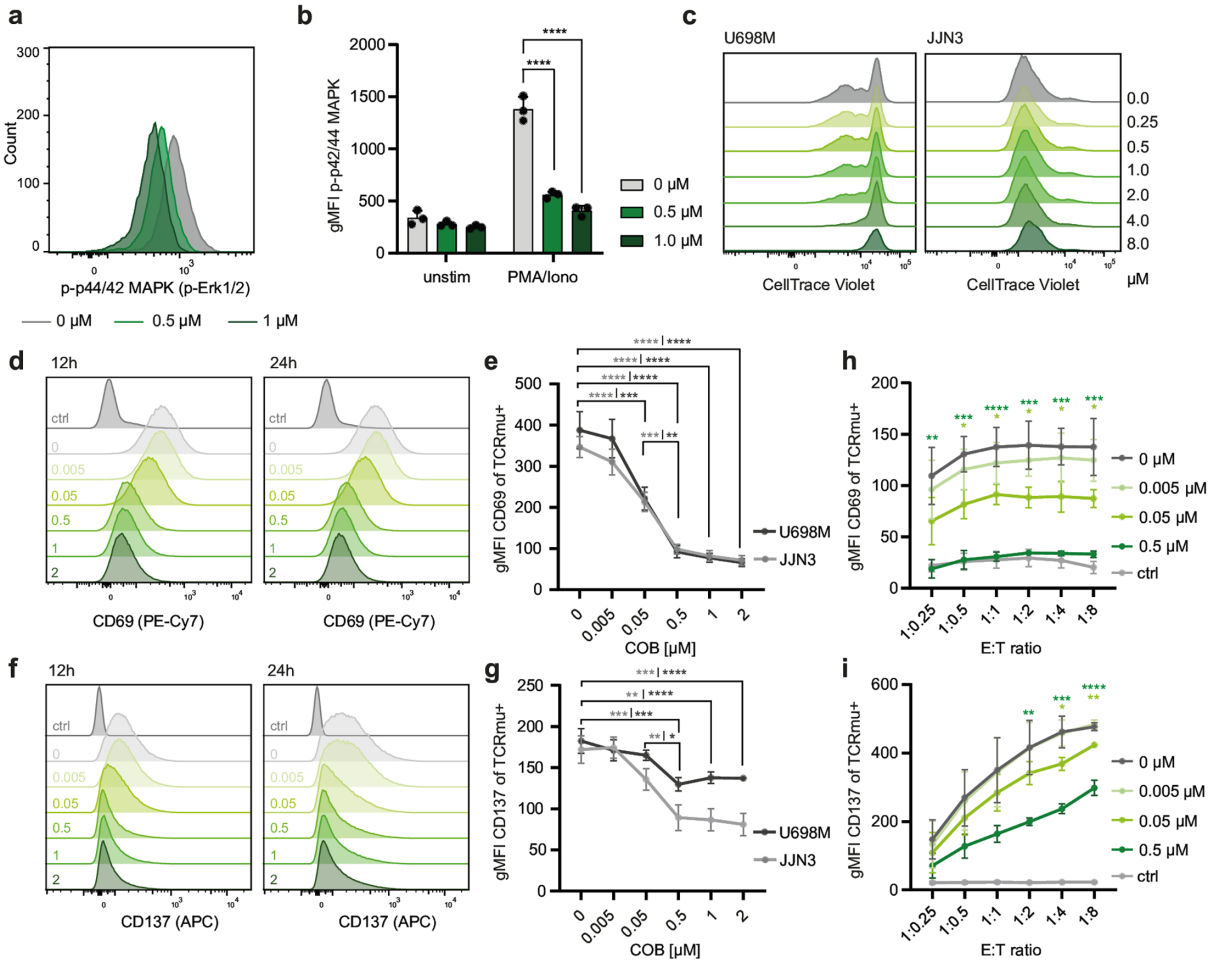

Figure 1 Decrease of T cell activation level following MEK inhibitor (MEKi) treatment. (a) Representative flow cytometry plot of intracellular levels of phospho (p)-p42/44 (p-Erk1/2) on increasing doses of cobimetinib (COB) after unspecific T cell activation via phorbol 12-myristate 13-acetate (PMA)/ionomycin (Iono). One-way analysis of variance (ANOVA) with Tukey's multiple comparison test: ****p<0.0001. (b) Flow cytometry-based geometric mean fluorescence intensity (gMFI) of p-p42/44 (p-Erk1/2) after PMA/Iono stimulation or without stimulation (unstim) in CD8+ T cells of three healthy donors. Mean and SD depicted. (c) Representative flow cytometry plots of CellTrace Violet (CTV)-labeled tumor cell lines U698M and JJN3 after 4 days of cultivation at increasing doses of COB (0–8 µM). (d–g) Extracellular (EC) flow cytometry staining of activation markers CD69 (d, e) and CD137 (f, g) after 12 hours (d left, f left) or 24 hours (d right, e, f right, (g) co-culture of KIF-sc1-tg CD8+ T cells with U698M-mut mg (effector-to-target (E:T) ratio 1:1) with increasing doses of COB (0, 0.005, 0.05, 0.5, 1, 2 µM). gMFI for both activation markers is shown. Representative flow cytometry plots after 12 hours and 24 hours of one (d, f) of three biological replicates (e, g, mean and SD after 24 hours) are depicted. Unstimulated control (ctrl) shown for all flow cytometry plots. One-way ANOVA with Tukey's correction for multiple comparisons; colors indicate cell line for which the test was performed: *p<0.05, **p<0.01, ***p<0.001, ****p<0.0001. (h, i) Extracellular (EC) flow cytometry staining of CD69 (h) and CD137 (i) after 20 hours co-culture of CD8+ KIF-sc1-tg T cells with U698M-mut mg at increasing doses of COB across increasing E:T ratios. Mean and SD of gMFI for three biological replicates are shown. One-way ANOVA with Tukey's correction for multiple comparisons; colors indicate comparison between 0.05 or 0.5 µM COB and 0 µM condition: *p<0.05, **p<0.01, ***p<0.001, ****p<0.0001.

classical T cell activation markers CD69 (figure 1d,e) and CD137 (figure 1f,g) on TCR-tg (TCRmu+) cells after 12 and 24 hours of co-culture and detected a dose-dependent decrease of both markers, suggesting a decrease in activation on MEKi treatment added from the beginning of co-culture. The addition of 0.5 µM COB already resulted in maximal decrease of CD137 and CD69 expression, suggesting strong inhibitory modulation of TCR-tg T cell activation (figure 1d–g). When examining the dose range below 0.5 µM and titrating the number of target cells per condition, the inhibitory effect of MEKi on T cell activation markers remained consistently detectable across the full range of tested E:T ratios at an early and a later time point (figure 1h,i, online supplemental figure S1a-j). In the context of early activation, inhibitory markers behaved as activation markers exhibiting lower surface levels following increasing doses of COB (online supplemental figure S1d, e, i, j, k-n). While canonical markers distinguishing memory subsets (CD45RA/CD45RO) were not affected by MEKi addition (online supplemental figure

Journal for ImmunoTherapy of Cancer: first published as 10.1136/jitc-2025-012800 on 1 December 2025. Downloaded from https://jitc.bmj.com on 12 February 2026 by guest. Protected by copyright, including for uses related to text and data mining, AI training, and similar technologies.

S1o), MEKi-treated T cells retained slightly higher levels of markers associated with a naïve phenotype (CD62L, CCR7) (online supplemental figure S1p). General trends of surface expression patterns of phenotypic markers were maintained up to day 4, whereas overall activation levels declined (online supplemental figure S1q–v).

Overall, we found that MEKi decreased TCR-tg T cell activation levels on both antigen-independent activation and encounter of tumor cells. Based on these findings, we defined the dose range for subsequent experiments, referring to 0.05 µM COB as low-dose and 0.5 µM as high-dose MEKi.

Low-dose MEKi during early T cell activation confers a quantitative advantage in T cell persistence on strong antigenic challenge

Beyond the observation that MEKi decreases TCR-T cell activation (figure 1, online supplemental figure S1), we next investigated the effect of this inhibitory modulation on TCR-tg T cell fitness, functionality, and survival. To test this, we set up further in vitro co-cultures with KIF-sc1-tg CD8+ T cells and U698M-mut mg or U698M-wt mg. Again, we employed different E:T ratios to simulate increasing tumor load and stimulation strength of TCR-T cells with increasing target counts. After the first 20 hours of co-culture, all KIF-sc1-tg T cells decreased in absolute count compared with the unstimulated wt mg-condition, independently of MEKi treatment or dose (figure 2a). Despite the inhibitory effect of MEKi on T cell activation, all conditions cleared the tumor with equal potency, although killing efficacy was strongly dependent on the E:T ratio (figure 2b).

After 96 hours of co-culture, MEKi-treated conditions differed significantly in their absolute TCRmu+ count compared with the untreated condition: while the maximum of residing TCRmu+ T cells was detected for low E:T ratios (1:0.25 and 1:0.5) for the untreated condition, highest TCRmu+ T cell counts for MEKi-treated conditions were detected for high E:T ratios (1:2 and 1:4, figure 2c). Overall, MEKi treatment shifted the optimum of TCR-tg T cell counts on tumor encounter, reflecting T cell fitness and survival, towards higher tumor load and therefore stronger T cell stimulation. Moreover, low-dose MEKi (0.05 µM) demonstrated significantly improved tumor cell killing at the optimum of TCR-tg T cell persistence (1:4, figure 2d). Compared with the addition of MEKi at a later time point (12 hours after co-culture set-up), low-dose MEKi from the beginning of co-culture (0 hour) still demonstrated a stronger effect on persisting TCR-tg T cells and tumor killing (figure 2e–h, online supplemental figure S2a-g). Significantly increased T cell persistence and tumor killing, along with decreased activation levels, were also observed for repeated stimulations of TCR-T cells over several days (online supplemental figure S2a-y). Notably, the degree of donor-dependent biological variability of tumor killing on addition of high-dose MEKi (figure 2h, online supplemental figure S2c, i, o, u) underlined the sensitivity of this system towards overly strong inhibitory modulation and the fine-tuned balance of T cell activation between understimulation and overstimulation.

To understand factors affecting T cell persistence on tumor encounter, we investigated activation-induced cell death and T cell proliferation. Concerning the first, we did not detect significant differences in apoptotic cell rates before the visible onset of cell proliferation after 20 hours of co-culture, despite the observation of lower T cell counts across all stimulated conditions (figure 2i,j), confirming our previous experiments (figure 2a). To investigate T cell proliferation, we tracked cell divisions and detected increased proliferation of T cells treated with low-dose MEKi at higher E:T ratios (figure 2k and online supplemental figure S3). However, an increase to high MEKi doses led to adverse effects decreasing proliferation, particularly on lower E:T ratios (figure 2k and online supplemental figure S3). Conclusively, the quantitative advantage of T cells observed with low-dose MEKi co-treatment is at least partially attributable to a proliferative benefit (figure 2k and online supplemental figure S3).

T cell performance benefits from MEKi co-treatment across diverse receptors and models, dependent on initial stimulation strength

To validate these findings further, we tested our hypothesis for different neoTCRs. By retroviral transduction, we genetically engineered healthy donor CD8+ T cells to express further neoTCRs from the oligoclonal TCR repertoire of patient Mel15[9–11] and activated them in co-culture with U698M-mut mg (online supplemental figure S4a-h). Low-dose MEKi improved T cell survival (figure 2l–n) without compromising cytotoxic capacity (online supplemental figure S4i-k). This advantage depended on the stimulation strength of each neoTCR construct, measured in part by functional avidity.[11] Low-dose MEKi demonstrated the strongest positive effects on T cell survival for neoTCR constructs with higher functional avidity (KIF-sc1, SYT-P1, and SYT-T1).[11] Meanwhile, neoTCRs with lower intrinsic stimulation potential (KIF-P1, KIF-P2, and KIF-sc2) only profited, if at all (see KIF-P1), at higher E:T ratios from low-dose MEKi (figure 2l–n). Interestingly, high-dose MEKi highlighted the complex dynamics within these T cell-tumor interactions, partly reversing these patterns (figure 2l–n) and also slightly decreasing killing ratios (online supplemental figure S4k). In summary, low-dose MEKi conferred the most pronounced benefit to strongly activated TCR-T cells.

To circumvent the artificial nature of TCR overexpression in virally engineered TCR-T cells, we continued to engineer TCR-T cells orthotopically by inserting the TCR-construct KIF-sc1 into the endogenous TRAC-locus via CRISPR/Cas9 as described previously.[11 33 34] TCR-T cells undergoing OTR profited similarly to retrovirally engineered TCR-T cells from low-dose MEKi. After 96 hours of co-culture, OTR-TCR-T cells showed significantly

Journal for ImmunoTherapy of Cancer: first published as 10.1136/jitc-2025-012800 on 1 December 2025. Downloaded from https://jitc.bmj.com on 12 February 2026 by guest. Protected by copyright, including for uses related to text and data mining, AI training, and similar technologies.

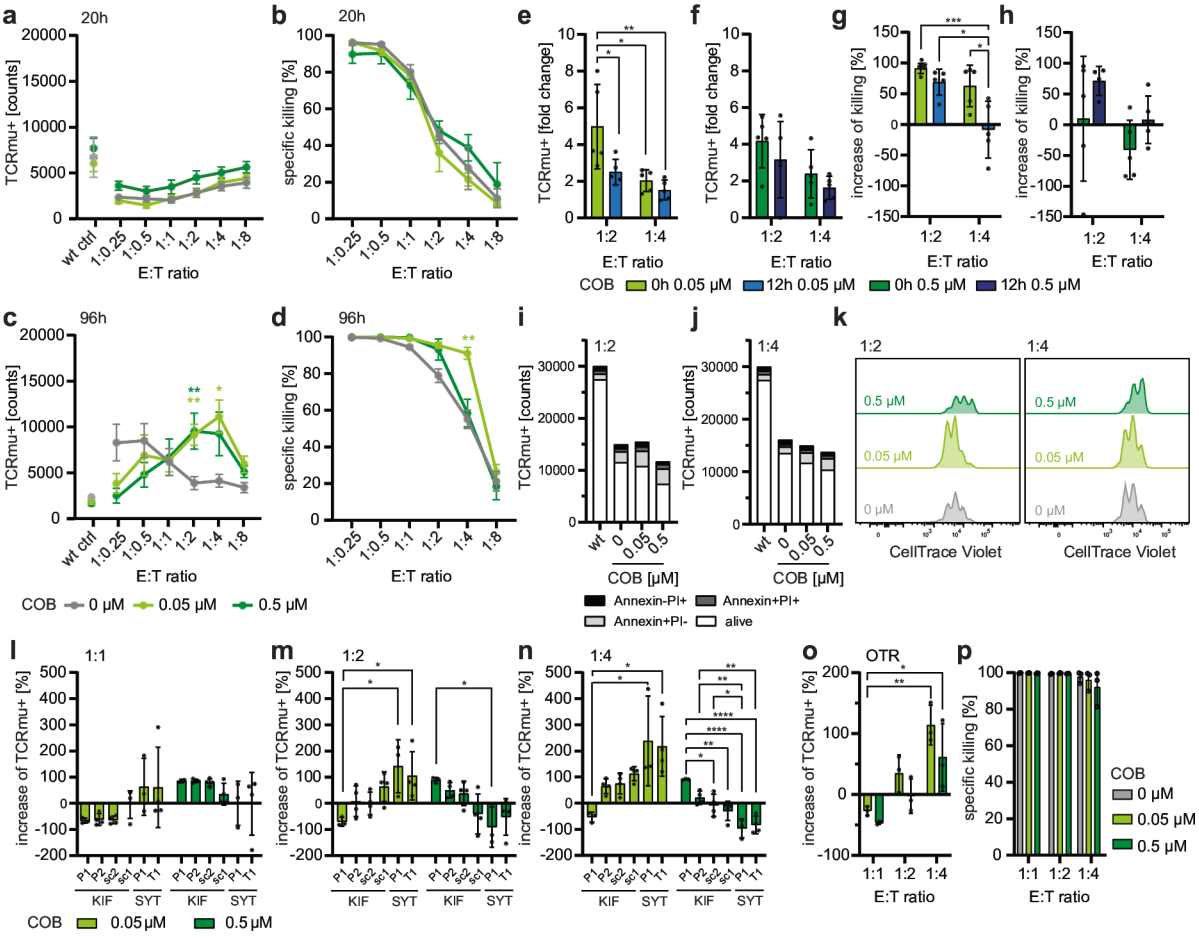

Figure 2 Low-dose MEK inhibition (MEKi) increases T cell performance in vitro by enhancing proliferation. (a-d) Flow cytometry-based quantification of CD8+ T cell receptor (TCR)-transgenic (tg) (TCRmu+) T cells and dsRed+ tumor cells after 20 hours (a, b) or 96 hours (c, d) co-culture of KIF-sc1-tg T cells with U698M-mut mg at increasing effector-to-target (E:T) ratios. U698M-wild-type (wt) mg served as unstimulated background control in E:T 1:4 (wt control (ctrl)). 0, 0.05, and 0.5 µM cobimetinib (COB) were compared with each other. Number of TCR-tg (TCRmu+) T cells is shown as absolute counts (a, c), specific killing is shown as percent killing compared with control condition with an unspecific TCR (2.5D6). Mean and SEM are depicted for five biological replicates. One-way analysis of variance (ANOVA) with Tukey's correction for multiple comparisons: *p<0.05, **p<0.01 (color indicates the COB concentration compared with 0 µM COB; only selected p values reported). (e-h) Fold-change of TCRmu+ KIF-sc1-tg (e, f) and increase of killing (g, h) each compared with the condition without COB co-treatment in a co-culture of KIF-sc1-tg T cells and U698M-mut mg (E:T 1:2 or 1:4). Mean and SD of five biological replicates per group are depicted. One-way ANOVA with Tukey's correction for multiple comparisons: *p<0.05, **p<0.01, ***p<0.001. (i, j) Annexin V-staining/propidium iodide (PI)-staining after 20 hours co-culture (KIF-sc1-tg T cells and U698M-mut mg) at different E:T ratios (i 1:2, j 1:4). U698M-wt mg (wt) served as unstimulated background control. Mean from three biological replicates depicted as absolute counts of TCRmu+ T cells per group. (k) Representative flow cytometry plots from one biological replicate of CellTrace Violet (CTV)-labeled CD8+ TCRmu+ T cells (KIF-sc1-tg) after 4 days of co-culture with U698M-mut mt at increasing doses of COB (0, 0.05, 0.5 µM). Comparison of different E:T ratios (left 1:2, right 1:4). (l-n) Increase of CD8+ T cells expressing different neoTCRs (in order of increasing functional avidity) from the repertoire of patient Mel 15[11] after 4 days of co-culture with U698M-mut mg at different E:T ratios (l 1:1, m 1:2, n 1:4). Percent increase of CD8+ T cells is shown for 0.05 and 0.5 µM COB in comparison with 0 µM COB. Mean and SD of four biological replicates are depicted. One-way ANOVA with Tukey's correction for multiple comparisons: *p<0.05, **p<0.01, ****p<0.0001. (o) Increase of CD8+ T cells in orthotopic TCR replacement (OTR)-engineered KIF-sc1-expressing T cells after 4 days of co-culture with U698M-mut mg. Percent increase of CD8+ T cells is shown for 0.05 and 0.5 µM COB in comparison with 0 µM COB. Mean and SD of three biological replicates are depicted. One-way ANOVA with Tukey's correction for multiple comparisons: *p<0.05, **p<0.01. Only selected p values reported. (p) Killing of U698M-mut mg within co-cultures of OTR-KIF-sc1-expressing T cells. Specific killing is shown as percent killing compared with a control condition with an unspecific TCR (against SARS-CoV-2). Mean and SD of three biological replicates are depicted.

increased T cell counts at higher E:T ratios, while maintaining equally potent tumor lysis (figure 2o,p).

We further compared our results from virally engineered T cells with another cell line, the MM cell line JJN3 B27-mut mg, which was also genetically engineered for the presentation of KIF2C^{P13L}. We detected comparable levels of T cell activation on tumor encounter of either U698M-mut mg or JJN3 B27-mut mg (online

Journal for ImmunoTherapy of Cancer: first published as 10.1136/jitc-2025-012800 on 1 December 2025. Downloaded from https://jitc.bmj.com on 12 February 2026 by guest. Protected by copyright, including for uses related to text and data mining, AI training, and similar technologies.

supplemental figure S4l-o), while MM cells were overall more susceptible to TCR-T cell-mediated tumor lysis (online supplemental figure S4p and q). Following MEKi, we detected increased TCR-tg T cells, again with the most substantial advantages for T cell performance for low-dose MEKi (optimum at E:T 1:5 (online supplemental figure S4r-u). Thus, MEKi demonstrated even stronger positive effects in the MM model compared with the lymphoma model (online supplemental figure S4r-u).

Due to the clinical importance of CAR-T cell treatments, we also tested our hypothesis on T cells expressing a CD19-directed CAR construct[32] (online supplemental figure S5a-d). While the addition of MEKi led to an increase in CAR-T cell numbers, depending on the CAR-construct (online supplemental figure S5a and c), killing rates were slightly decreased for CAR-T cells on MEKi (online supplemental figure S5b and d). These findings underscore the strong dependency of the co-treatment effect on the individual receptor and its stimulation strength. In our model system, this translated into a more pronounced benefit for TCR-T cells compared with CAR-T cells.

To validate this co-treatment concept beyond engineered T cells, we tested the addition of COB to co-cultures employing a bispecific T cell engager (BiTE) as another clinically relevant therapeutic regime. We therefore added an anti-EGFR-anti-CD3 BiTE[41] to co-cultures of non-engineered CD8+ T cells and the lung cancer cell line A549, which was itself highly sensitive to the addition of MEKi (online supplemental figure S5e). Confirming our previous findings, low-dose MEKi resulted in an increase of CD8+ T cells in a dose-dependent manner of the added BiTE (online supplemental figure S5f and g) at a slightly increased proliferative rate as indicated by CTV staining (online supplemental figure S5h) and comparable tumor killing rates (online supplemental figure S5i). A similar analysis adding MEKi to anti-CD19-anti-CD3 BiTE blinatumomab in co-culture with U698M B cell lymphoma revealed an even stronger advantage for T cell persistence (online supplemental figure S5j-m) and tumor killing (online supplemental figure S5n and o).

To explore the proliferative advantage of MEKi treatment for tumor-infiltrating lymphocytes (TILs), we reanalyzed one of the few published sequencing datasets on MEKi-treated T cells derived from primary patient material. Lim *et al* applied single-cell RNA sequencing to investigate immunotherapy-naïve and immunotherapy-resistant melanoma tumor lysates in response to 48 hours ex vivo BRAF inhibitor dabrafenib and MEKi trametinib (DT) treatment.[42] We reanalyzed this published dataset, performing unbiased clustering on the immune cells (online supplemental figure S6a and b). While cluster 5 (CD8+ cytotoxic T cells) exhibited the highest expression level of selected activation markers, TCR-specific signaling (mainly detected by *NR4A1*) remained low across all T cells (online supplemental figure S6c), most likely due to low levels of tumor-specific activation. To assess the effect of the treatment on the different immune cell clusters, we calculated an expression score based on a gene list indicating MAPK pathway activation by Pratilas *et al*[43] as used for analysis in the original study on the dataset.[42] This analysis showed only low overall MAPK activity across immune cell clusters and only a slight but consistent decrease in MAPK activity on DT treatment (online supplemental figure S6d). Meanwhile, transcripts indicating T cell proliferation (GO:0042098) were slightly upregulated per cluster on DT treatment (online supplemental figure S6e). Pathway enrichment analysis within all cytotoxic CD8+ T cells (cluster 5) supported these data as pathways involved in G2/M transition and mitosis were specifically upregulated on DT treatment (online supplemental figure S6f) while T cell activation was attenuated, indicated by the decrease of genes involved in interferon signaling, CD28 co-stimulation, and TCR signaling (online supplemental figure S6g).

Overall, our findings across various models, employing different receptors, activation strengths, engineering strategies, and distinct tumor cell lines, as well as analyses of publicly available data, including non-engineered, tumor-derived CD8+ T cells, reinforce the benefit of MEKi co-treatment on T cell fitness and proliferation. These results also underscore the dependency on the strength of T cell stimulation, highlighting the advantage of moderate activation as a critical determinant of T cell performance.

Low-dose MEKi enhances TCR-tg T cell-mediated tumor killing in vivo

Considering the seemingly narrow treatment window of MEKi in vitro, we sought to investigate the effect of MEKi in an established in vivo xenograft model[10 11] to test for treatment relevance in a more physiological 3D-T cell-tumor cell interaction (figure 3a, online supplemental figure S7a). First, the injection of MEKi, even at a high dose, did not affect tumor cell growth of U698M-mut mg per se when tested in combination with a control TCR 2.5D6 (online supplemental figure S7a-d). Furthermore, the high dose of COB (7.5 mg/kg bw) did not significantly improve tumor control and survival in vivo when combined with the injection of tumor-specific KIF-sc1-tg T cells (online supplemental figure S7e-g). In parallel to the previous in vitro observations, lowering the MEKi dose (1 mg/kg bw) resulted in a significant decrease in tumor outgrowth (figure 3b,c, online supplemental figure S8a and b) and a significant improvement of survival over time (figure 3d). CD8+ T cells derived from tumors at early time points after T cell injection showed no significant differences in tumor-infiltrating T cells (figure 3e, f and g), T cell activation patterns, memory phenotype, or stemness markers (figure 3h,i, online supplemental figure S8c-k)—despite induction of T cell activation compared with splenic T cells (online supplemental figure S8l-t)—and both treatment conditions exhibited homogeneous T cell infiltration across the tumor

Journal for ImmunoTherapy of Cancer: first published as 10.1136/jitc-2025-012800 on 1 December 2025. Downloaded from https://jitc.bmj.com on 12 February 2026 by guest. Protected by copyright, including for uses related to text and data mining, AI training, and similar technologies.

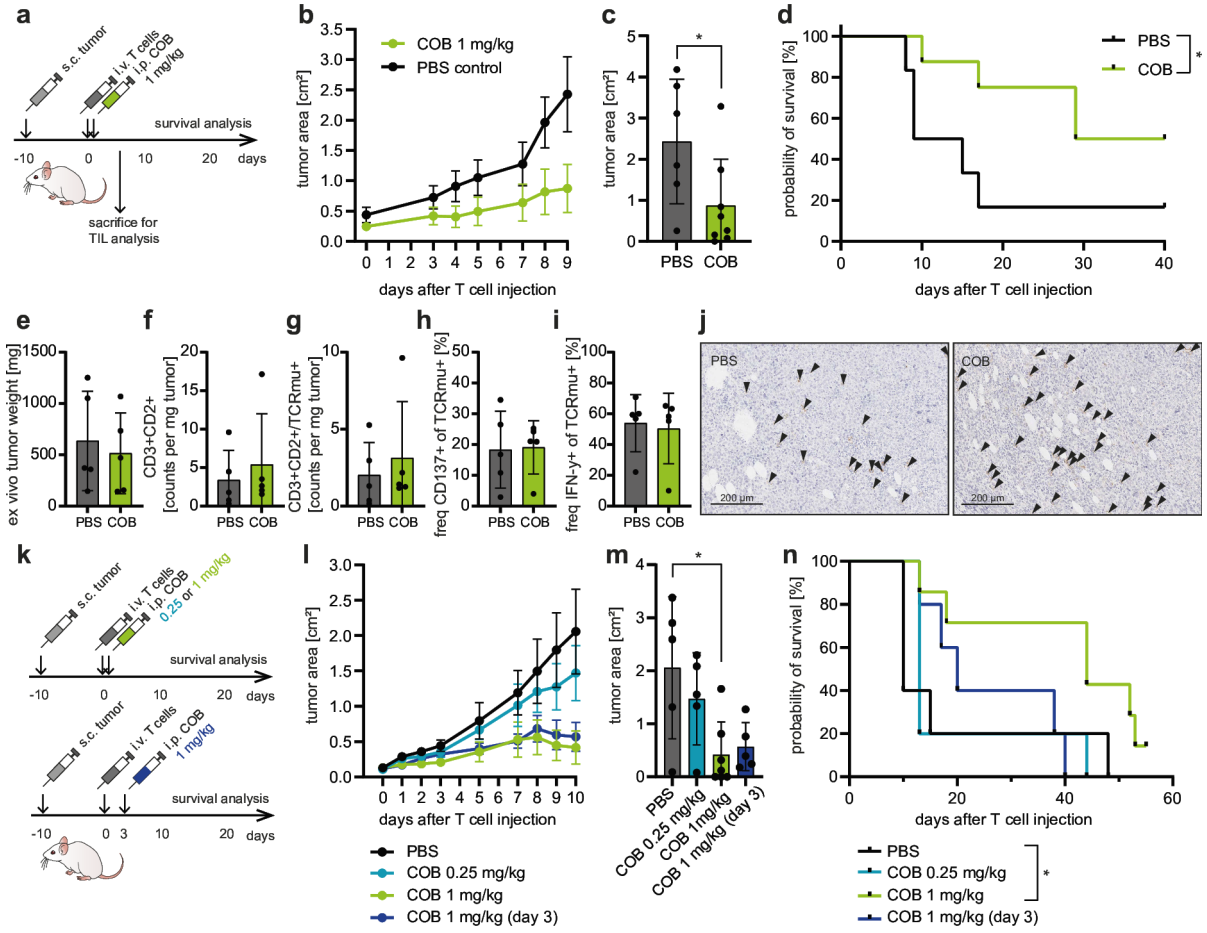

Figure 3 Low-dose MEK inhibition (MEKi) enhances tumor control by adoptively transferred T cell receptor (TCR)-transgenic CD8+ T cells in vivo. (a) Schematic representation of in vivo xenograft model in tumor-bearing (U698M-mut mg) NSG mice with simultaneous injection of TCR-T cells (intravenous (i.v.)) and cobimetinib (COB) at 1 mg/kg body weight (bw) (intraperitoneal (i.p.)) on day 0. (b) Tumor area of tumor-bearing NSG mice in cm^2 as measured by digital caliper after injection of TCR-T cells and COB. All mice received subcutaneous (s.c.) injection of 10×10^6 U698M-mut mg tumor cells on day −10 and i.v. 3×10^6 KIF-sc1-transgenic (tg) T cells on day 0, as well as either i.p. injection of 1 mg/kg bw COB (n=8) or phosphate-buffered saline (PBS) (n=6). Mean and SEM depicted per group. (c) Tumor area on day 9 after T cell injection comparing COB (n=8) vs PBS (n=6) group. Mean and SD shown. Unpaired t-test: *p<0.05. (d) Probability of survival until day 40 after T cell injection comparing COB (n=8) vs PBS (n=6) tumor-bearing NSG mice. Mantel-Cox test: *p<0.05. (e) Ex vivo tumor weights in mg at day 5 after T cell injection. Mean and SD shown. (f-i) Flow cytometry analysis of tumor-infiltrating lymphocytes (TILs) from NSG mice sacrificed on day 5 after T cell injection and i.p. 1 mg/kg bw COB (n=5) or PBS (n=5). Mean and SD are depicted for T cell counts and frequency of CD137+ (extracellular (EC)) or IFN-γ+ (intracellular (IC)) TCR-tg T cells derived from the tumor tissue. (j) Immunohistochemistry anti-CD8-staining of one representative tumor for the PBS (left) versus COB-treated (right) group (total n=5 per treatment). Arrows mark exemplary CD8+ cells in sections with 20× magnification. (k) Schematic representation of in vivo xenograft model in NSG mice with injection of U698M-mut mg, KIF-sc1-tg TCR-T cells (i.v.) and COB at 0.25 or 1 mg/kg bw on day 0 or 1 mg/kg bw on day 3 (i.p.). Comparison is made with mice receiving PBS (i.p.) in addition to KIF-sc1-tg T cells. (l) Tumor area of U698M-mut mg tumor-bearing NSG mice in cm^2 as measured by digital caliper after injection of TCR-T cells and COB on day 0 or day 3. All mice received 3×10^6 KIF-sc1-tg T cells on day 0 and either i.p. injection of 0.25 (n=5) or 1 mg/kg bw (n=6) COB on day 0 or 1 mg/kg bw (n=5) on day 3 or PBS (n=5). Mean and SEM depicted per group. (m) Tumor area on day 10 after T cell injection comparing all groups also shown in l. Mean and SD shown. One-way analysis of variance (ANOVA) with Tukey's correction for multiple comparisons: *p<0.05. (n) Probability of survival until day 55 after T cell injection comparing groups described in l. Mantel-Cox test: *p<0.05.

tissue (figure 3j, online supplemental figure S8u). Nevertheless, the stronger antitumor effect observed later suggests that MEKi enhances T cell persistence and functionality over time. Further decrease in COB concentration did not enhance tumor control or survival (figure 3k–n, online supplemental figure S8v-y). Similarly, delayed start of the treatment on day 3 after T cell injection did not result in a significant long-term survival benefit despite an initial effect on the tumor growth (figure 3k–n, online supplemental figure S8v-y). Thus, corresponding with our in vitro data, low-dose MEKi co-treatment from the beginning of T cell activation resulted in the most potent increase in T cell-dependent antitumor response.

Journal for ImmunoTherapy of Cancer: first published as 10.1136/jitc-2025-012800 on 1 December 2025. Downloaded from https://jitc.bmj.com on 12 February 2026 by guest. Protected by copyright, including for uses related to text and data mining, AI training, and similar technologies.

MEKi dampens inflammatory T cell activation signature, including loss of TNF secretion

We next aimed to functionally understand the advantage of low-dose MEKi co-treatment on the fitness of CD8+ TCR T cells. We co-cultured TCR-T cells for 20 hours or 96 hours with U698M-mut mg and analyzed the transcriptional profile of CD8+ cells. Differential gene expression of all samples collected after 20 hours of co-culture revealed decreasing immune activation and cytokine signaling with increasing COB dose (figure 4a). Comparing 0.05 µM with 0 µM COB (online supplemental figure S9a) as well as 0.5 µM with 0 µM COB (online supplemental figure S9b) separately stressed the downregulation of several genes linked to inflammatory immune responses already on low-dose MEKi co-treatment. Across all analyses, we found MEKi-dependent decrease of genes included in pathways like immune cytokine and IL signaling (*TIMP1, TNFSF14, IL23A, TRIM8, EGR1, CCL3, CCL4, CCL3L1, DUSP4, IFNG, PRF1*), signal transduction (eg, *CAV1, NTRK1, CKB, GZMB, RHOBTB3, CCL1, SH2D2A, FPSL1, GNAI1*) and MAPK family signaling cascades (*PDGFA, DUSP4, DUSP5, DUSP2, ETV4, SRED2*) (figure 4a, online supplemental figure S9a and b). After 96 hours of co-culture, differential gene expression analysis was consistent with significantly lower levels of immune cytokine signaling (*EBI3, EGR1, CD44, IL1RN*) with MEKi (online supplemental figure S9c). This state of reduced pro-inflammatory signaling of MEKi-treated CD8+ T cells was reflected by the significant downregulation of pathways like chemokine signaling, cytokine-cytokine-receptor interaction, and leukocyte migration (figure 4b,c, online supplemental figure S9d-g). MAPK—expectedly from the treatment—and NFκB signaling also ranked among the downregulated pathways (figure 4b,c). In parallel, MEKi-treated conditions were characterized by a sparse number of genes upregulated in their transcriptomic profile. Among these few, we detected variable genes involved in processes of T cell metabolism, signaling, trafficking, and differentiation, for example, *STMN1, ABCD2, HEBP2, PGM2L1, SESN3, ACTN2, DGKH, PHKB, PLAGL1, PHLDB2, PRSS23* (figure 4a, online supplemental figure S9a and b).

Based on the observed reduction of pro-inflammatory signaling on MEKi, we analyzed the cytokine secretion profile by 13-plex assay of canonical CD8 T cell/natural killer cytokines (figure 4d–h, online supplemental figure S10a-m) to assess effector function. The addition of MEKi decreased the secretion of central effector cytokines such as IFN-γ, IL-2, TNF, GZMB, or perforin in a dose-dependent and E:T ratio-dependent manner (figure 4d–h, online supplemental figure S10a-q). One cytokine, TNF, showed a surprisingly strong response to the presence of MEKi, with almost complete abrogation of TNF secretion already at low-dose MEKi (figure 4f, online supplemental figure S10f). We could confirm this decrease in expression of *IFNG, IL2, TNF, GZMB,* and *PRF1* transcripts after 20 hours (figure 4i–m), again with a sudden drop for TNF transcripts already on low-dose COB conditions (figure 4k). Surprisingly, compared with the other cytokines, the secretion of granulysin (GNLY) increased on MEKi, possibly enhancing effector function (online supplemental figure S10m and q). After 96 hours of co-culture, most canonical CD8 effector cytokines analyzed showed substantially decreased transcriptomic expression (figure 4i–l) except for *PRF1* (figure 4m).

Overall, we observed a gradual, strong reduction of pro-inflammatory signaling on MEKi treatment, evident at the transcriptomic level and even more markedly at the protein level. This included a near-complete loss of TNF secretion, which emerged as a key functional consequence.

MEKi abrogates NFκB-promoter and NFAT-promoter activity in addition to decreasing Erk1/2-phosphorylation

To explore the mechanistic basis of this decrease in the pro-inflammatory signature, particularly the loss of TNF secretion, we investigated key elements of TCR signaling. Therefore, we employed a TPR platform, JE6.1 Jurkat T cells for AP-1, NFAT, and NFκB[36] completed with CD8α and CD8β chains[37] and our neoTCR of interest. For specific activation, we co-cultured these reporter cells with different antigen-expressing cell lines, U698M-mut mg (figure 5a–c) and JJN3 B27-mut-mg (online supplemental figure S11a-c). Longitudinal flow cytometric analysis within the first 24 hours of co-culture revealed a marked decrease in AP-1 reporter activity, a surrogate for the MAPK pathway. MEKi particularly took effect after the first 4 hours of T cell-tumor interaction (figure 5a, online supplemental figure S11a). Surprisingly, the activity of the reporters for NFκB and NFAT was completely abrogated by the addition of 0.5 µM COB (figure 5b,c, online supplemental figure S11b and c). We next aimed to exclude substance-specific effects of COB. Testing this setup with four additional MEK1/2-specific inhibitors, SELU, BINI, GDC, and TRA, revealed a similar picture for signaling activity (figure 5d, online supplemental figure S11d). While, depending on the inhibitor dose, AP-1 activity was significantly reduced on MEKi, we detected near-complete abrogation of the activity of NFκB and NFAT reporters (figure 5e–g) across different neoTCRs tested (online supplemental figure S11e-g). Unspecific PMA/Iono stimulation did not alter the pattern of NFκB and NFAT activity, whereas the reduction in AP-1 activity was more pronounced compared with TCR-specific stimulation (figure 5h–j, online supplemental figure S11h-j). In primary CD8+ T cells (online supplemental figure S12a-c) as well as TPR JE6.1 CD8+ Jurkat cells (online supplemental figure S12d-f), we could recapitulate the decrease of phospho-p42/44 (p-ERK1/2) downstream MEK, the target of MEKi COB (online supplemental figure S12a and b). Early phosphorylation events of IκBα and p65 within the NFκB pathway (online supplemental figure S12b and e) and NFAT dephosphorylation (online supplemental figure S12c and f), however, remained intact despite the eventual loss of reporter activity, suggesting that MEKi

Journal for ImmunoTherapy of Cancer: first published as 10.1136/jitc-2025-012800 on 1 December 2025. Downloaded from https://jitc.bmj.com on 12 February 2026 by guest. Protected by copyright, including for uses related to text and data mining, AI training, and similar technologies.

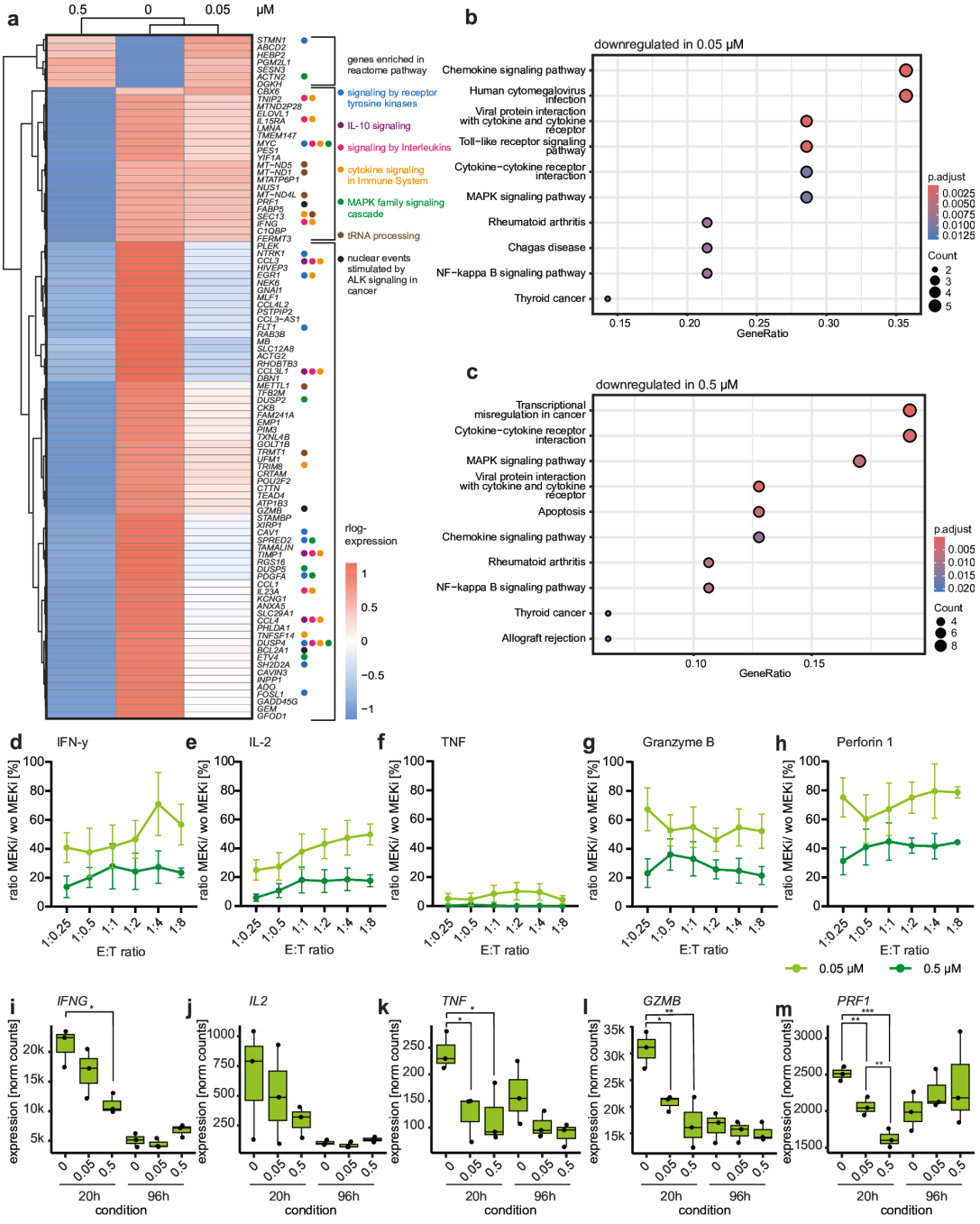

Figure 4 MEK inhibition (MEKi) decreases inflammatory profile of engineered T cells on a transcriptomic and functional level. (a) Hierarchically clustered heatmap of rlog-transformed expression of all genes significantly differentially expressed (adjusted p value (padj)<0.05) between CD8-T cell conditions after 20 hours co-culture with U698M-mut mg (differentially expressed gene analysis of all 20 hours samples). Mean rlog expression of three biological replicates is shown. Major clusters were marked manually on the right side. Enriched genes were marked manually according to their enrichment in selected Reactome-pathways (color code in the figure). (b, c) Kyoto Encyclopedia of Genes and Genomes pathway geneset enrichment analysis of differentially downregulated pathways in 0.05 µM (b) and 0.5 µM (c) cobimetinib (COB) compared with 0 µM COB after 20 hours of co-culture. Pathways were considered significant at padj<0.05. (d-h) 13-plex analysis of classical effector cytokines (d interferon (IFN)-γ, e interleukin (IL)-2, f tumor necrosis factor (TNF), g granzyme B, h perforin 1) of CD8-T cell response from the supernatant of 20 hours co-culture of KIF-sc1-tg T cells and U698M-mut mg target cells (quantitative dynamics of the experiment shown in figure 2a–d). Ratio of cytokine concentration on COB addition is shown in comparison to 0 µM COB. Mean and SD of five biological replicates. (i-m) Expression of cytokine RNA transcripts in bulk RNA sequencing (RNA-seq) analysis from CD8+ T cells (MACS-enriched) after 20 hours or 96 hours of co-culture with U698M-mut mg (effector-to-target (E:T) ratio=1:4). Increasing doses of COB were compared as depicted on the x-axis: 0, 0.05, and 0.5 µM at both time points. Mean and minimum to maximum of normalized counts shown for three biological replicates. One-way analysis of variance (ANOVA) with Tukey's correction for multiple comparisons comparing samples within 20 hours or 96 hours time point: *p<0.05, **p<0.01, ***p<0.001. MAPK, mitogen-activated protein kinase; NF, nuclear factor.

Journal for ImmunoTherapy of Cancer: first published as 10.1136/jitc-2025-012800 on 1 December 2025. Downloaded from https://jitc.bmj.com on 12 February 2026 by guest. Protected by copyright, including for uses related to text and data mining, AI training, and similar technologies.

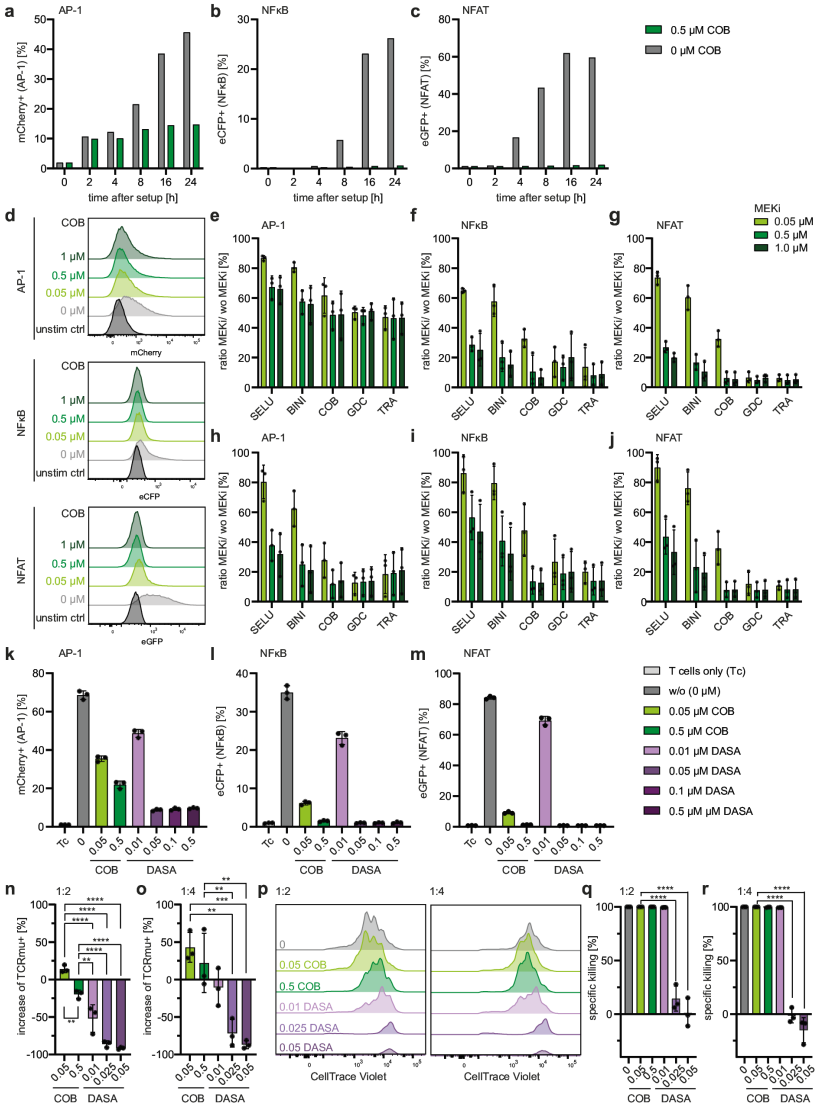

Figure 5 MEK inhibition (MEKi) acts by selective complete inhibition of nuclear factor kappa-light-chain-enhancer of activated B cells (NFκB) and nuclear factor of activated T cells (NFAT) and partial inhibition of activator protein 1 (AP-1) signaling. (a-c) Time course over 24 hours of reporter activity for AP-1 (MCherry fluorescent protein (mCherry)), NFκB (enhanced cyan fluorescent protein (eCFP)), and NFAT (enhanced green fluorescent protein (eGFP)) in JE6.1 triple parameter reporter (TPR) CD8+ KIF-sc1-tg Jurkat cells upon co-culture with U698M-mut mg (effector-to-target (E:T) ratio 1:1) comparing condition without (0 µM) and with 0.5 µM cobimetinib (COB). One representative of three experiments is shown. (d) Representative flow cytometry plots of mCherry, eCFP, and eGFP expression (co-culture setup described in a) with further concentrations of COB (0, 0.05, 0.5, and 1 µM). Comparison is made to an unstimulated control (unstim ctrl) condition. (e-j) Ratio of reporter activity (mCherry, eCFP, and eGFP) in conditions with MEKi compared with 0 µM MEKi after 20 hours co-culture between JE6.1 TPR CD8+ KIF-sc1-Jurkat T cells and either specific stimulation via U698M-mut mg (E:T=1:1, e–g) or unspecific stimulation with phorbol 12-myristate 13-acetate (PMA)/ionomycin (Iono) (h–j) at increasing doses of five different MEKi: selumetinib (SELU), binimetinib (BINI), COB, GDC-0623 (GDC), trametinib (TRA). Mean and SD of three independent experiments are shown. (k-m) Flow cytometry-based measurement of reporter activity for AP-1 (mCherry), NFκB (eCFP), and NFAT (eGFP) in JE6.1 TPR CD8+ KIF-sc1-tg Jurkat T cells on co-culture with U698M-mut mg (E:T 1:1) after 24 hours. T cells only (Tc) conditions served as unstimulated background control. Increasing doses of COB (green) were compared with dasatinib (DASA, violet). Mean and SD of experimental triplicates are depicted. (n, o) Flow cytometry-based quantification of T cell receptor (TCR)mu+ T cells after 96 hours of co-culture of KIF-sc1-tg T cells and U698M-mut mg (E:T 1:2 (n) or 1:4 (o) as indicated above graphs). Percent increase or decrease of TCR-transgenic (tg) T cells compared with conditions without inhibitor (0 µM) is depicted for COB-treated or DASA-treated conditions (concentrations in µM). Mean and SD for three biological triplicates are shown. One-way analysis of variance (ANOVA) with Tukey's correction for multiple comparisons: **p<0.01, ***p<0.001, ****p<0.0001. (p) CellTrace Violet (CTV)-flow cytometry plots from one representative of three donors comparing increasing doses of COB and DASA with 0 µM condition without inhibitor. (q, r) Flow cytometry-based quantification of dsRed+ tumor cells after 96 hours of co-culture of KIF-sc1-tg T cells and U698M-mut mg (E:T 1:2 (q) or 1:4 (r) as indicated above graphs). Per cent killing is depicted compared with unspecific control TCR 2.5D6. Mean and SD for three biological triplicates are shown. One-way ANOVA with Tukey's correction for multiple comparisons: ****p<0.0001. Only significant p values for comparisons with 0.05 µM COB are depicted.

Journal for ImmunoTherapy of Cancer: first published as 10.1136/jitc-2025-012800 on 1 December 2025. Downloaded from https://jitc.bmj.com on 12 February 2026 by guest. Protected by copyright, including for uses related to text and data mining, AI training, and similar technologies.

interferes with downstream regulatory layers of gene expression.

Selective transcriptional inhibitory profile of MEKi compared with tyrosine kinase inhibitor dasatinib exhibits a significant advantage for T cell persistence

The tyrosine kinase inhibitor DASA was previously used as an off-switch to CAR-T cells in vitro and in vivo,[20 21] suggesting potential to temper TCR-T cell activation in low doses similar to the suggested approach using MEKi. Therefore, we next compared the inhibitory signaling profile of MEKi COB with DASA for a better understanding of its relevance for the increase in T cell persistence. DASA impacted tumor growth significantly more strongly than MEKi (online supplemental figure S13a and b) and exhibited a near-complete loss of signaling activity across all three major T cell orchestrators at doses starting from 0.05 µM. Compared with MEKi COB, we could not detect residual reporter activity for the AP-1 pathway following addition of DASA (figure 5k–m, online supplemental figure S13c-f). This strong, less selective inhibitory effect of DASA was further reflected by significantly lower levels of activation marker expression on TCR-tg T cells, particularly after 20 hours (online supplemental figure S13g-l). Interestingly, while cells at 0.01 µM DASA had already downregulated CD137 expression after 96 hours, previously nearly non-activated T cells at a medium DASA concentration started to upregulate the activation marker (online supplemental figure S13j), suggesting a delicate balance of the inhibitory effects, potentially also dependent on the half-life of the inhibitor. In contrast to COB, the overly strong inhibitory effect of DASA resulted in a significant decrease in persisting TCR-T cells after co-culture (figure 5n,o, online supplemental figure S13m and n). This was further evidenced by a reduction in proliferative activity (figure 5p), as well as a decrease in killing capacity, particularly at higher DASA doses (figure 5q,r, online supplemental figure S13o and p)—although already noticeable at 0.01 µM (online supplemental figures S13o and p). Notably, the proliferative and quantitative disadvantage for T cell persistence following DASA was reported for all doses applied, including the lowest (0.01 µM), which neither influenced tumor growth nor led to a significant decrease in activation level and even sustained significantly higher reporter activity for AP-1, NFκB, and NFAT than the previously established MEKi co-treatment regime. These findings suggest a crucial role for the selective inhibitory profile of MEKi-dependent tempering of T cell activation, maintaining residual activity of AP-1.

In conclusion, MEKi treatment acts by complete disruption of NFκB and NFAT transcriptional activity, similar to DASA, and only partial disruption of AP-1, in contrast to DASA. Our data suggest that not the inhibition of T cell activity alone, but the MEKi-induced selective shift in the activity of major transcription factors during early T cell activation eventually induces the observed advantage on T cell fitness.

DISCUSSION

Our work suggests MEKi as a promising tool for slightly and selectively tempering the TCR-T cell activation profile towards a 'Goldilocks' point of T cell functionality and persistence. Depending on signal strength, a single, low dose of MEKi during the early phase of T cell activation shifted the optimum of TCR-tg CD8+ T cell proliferation and survival to stronger stimuli and higher tumor load, ultimately resulting in a quantitative and qualitative advantage in tumor control. This effect was demonstrated in vitro and in vivo, after multiple stimulation rounds of TCR-T cells, across a panel of neoTCRs with distinct activation signatures and functional avidities,[11] different cell lines, and different modes of T cell engineering (retroviral vs orthotopic TCR replacement).[33 34] We also include data on a similar advantage of low-dose MEKi in CAR-engineered T cells, as well as non-genetically altered CD8+ T cells directed towards the tumor via BiTEs. Furthermore, we report increased proliferative activity in primary tumor-infiltrating T lymphocytes after ex vivo addition of dabrafenib and trametinib.[42] Notably, MEKi exhibits a selective inhibitory profile, partially preserving AP-1 activity, which our data suggest is central to the increase in T cell persistence. We show for TCR-T cells that the positive effect on T cell fitness depends on the stimulus strength: strongly activated T cells profit significantly more from low-dose MEKi co-treatment.

Our findings across several model systems outline the delicate balance between overstimulation and understimulation that must be carefully engineered in ACT and potentially also further T cell-based immunotherapies. In a previous case study on the neoTCR repertoire of a patient with melanoma with complete response to ICI,[9–11] we demonstrated superior rechallenge capacity and persistence of TCR clonotypes with relatively more moderate TCR signal strength,[11] as also supported by further recent studies.[16 17 44 45] This concept of 'Goldilocks' CD8+ T cell activation[46–48] informed the combinatorial engineering approach for ACT suggested here. While prior preclinical combinatorial approaches in $BRAF^{V600}$ mouse melanoma models investigated the effect of MEKi on the tumor itself,[49 50] our work focused on the effect on TCR-T cells in a dose range too low to affect tumor growth.

Modulation of engineered T cell function has previously been studied using DASA, resulting in the prevention of exhaustion through tonic signaling[20] and CRS after in vivo application of CAR-T cells.[21] However, rather than the near-complete off-switch achieved with the Src tyrosine kinase inhibitor DASA to completely rest CAR-T cells,[20 21] we set up a therapeutic regimen designed for fine-tuning T cell signal strength towards slightly more tempered profiles during early activation.

Compared with other preclinical studies on MEKi,[26 27 31] lower and fewer doses resulted in the optimal effect on TCR-T cell fitness. This aligns with data from a murine KRAS-mutant non-small cell lung cancer study, where pulsatile MEKi treatment, rather than continuous dosing,

Journal for ImmunoTherapy of Cancer: first published as 10.1136/jitc-2025-012800 on 1 December 2025. Downloaded from https://jitc.bmj.com on 12 February 2026 by guest. Protected by copyright, including for uses related to text and data mining, AI training, and similar technologies.

triggered stronger antitumor T cell responses.[51] High doses of MEKi (≥0.5 µM COB in our models) caused T cell understimulation, reducing both antitumor activity and proliferation, also aligning with results from other studies.[52] Clinical studies combining antiprogrammed death-ligand 1 treatment with MEKi COB—NCT01988896 (different entities, n=152),[28] IMspire170 (melanoma, n=446)[29]—relied on the Food and Drug Administration-approved dosing schedule of 60 mg oral COB for 21 days followed by a 7-day treatment break. This regimen yields peak serum levels of 273 ng/mL (513.9 µM),[53] far exceeding the doses used in our study. Notably, neither trial showed significant clinical benefit, suggesting that prolonged exposure to high-dose MEKi may impair T cell function. Clinical evaluation of endogenous and adoptively transferred T cells in combination with low-dose MEKi will be essential to determine the potential of this approach outside preclinical immunodeficient xenograft models.

Aiming at a better understanding of the mechanistic effect of low-dose MEKi, we investigated the transcriptomic and functional activation signature of MEKi-treated TCR-T cells. Transcriptionally, we detected the downregulation of numerous genes involved in pro-inflammatory cellular responses; specifically, genes involved in chemokine-signaling (eg, *CCL3, CCL4, CCL4L2, CCL1, CCL3-AS1, CXCL13*) or cytokine response (eg, *IFNG, GZMB, IL3, IL23A, IL15RA, TNFSF14*). The decrease of canonical CD8 effector cytokines such as IFN-γ, IL-2, or GZMB after administration of low-dose MEKi supported the notion of a decreased inflammatory profile of CD8+ T cells. While inflammatory cytokines are necessary as the third signal in the classical model of T cell activation, overt inflammation impedes T cell memory formation[54] and increases CD8+ T cell contraction.[55] The MEKi-induced quantitative shift in the optimum of persisting T cells towards higher tumor load suggests an altered expansion and contraction phase of CD8+ T cell responses.

Of all cytokines assessed, TNF secretion was most profoundly reduced by MEKi, with levels nearly abolished—suggesting a protective role. TNF remains a double-edged molecule: while it is known as an inflammatory effector molecule enhancing CD8+ T cell-mediated tumor lysis,[56 57] it can simultaneously induce apoptosis, particularly in mature CD8+ T cells.[58] Consequently, blockade of TNF has been shown to overcome resistance to antiprogrammed death-1 (anti-PD-1) ICI, likely by preventing anti-PD-1-induced TIL cell death.[59]

Since *TNF* transcription is strongly controlled by NFκB signaling rather than MAPK signaling,[60] the complete abrogation of TNF expression on MEKi was unexpected. Investigations of TCR signaling on MEKi revealed near-complete loss of NFκB and NFAT reporter activity across experiments with five different MEKi. We further showed that early phosphorylation of the NFκB pathway remained unaltered on MEKi until phosphorylation of p65 (RelA). Earlier reports, mostly carried out in other cell types than activated T cells, confirmed that transcriptional activity, but not DNA binding of NFκB, was sensitive to inhibition of p38.[61–63] Similarly, early NFAT dephosphorylation was not affected by the addition of MEKi in our analyses. Since the early signaling events of both pathways remained intact, this suggests MEKi-dependent disruption of transcription factor binding, co-activator recruitment, chromatin accessibility, or post-transcriptional regulation.

Notably, the comparison with DASA exhibited a significantly more selective inhibitory profile of MEKi, nearly abolishing—like DASA—NFκB and NFAT activity, but—in contrast to DASA—partly preserving AP-1 activity. Compared with MEKi, even the lowest dose of DASA, maintaining significantly higher levels of reporter activity across all three major TCR signaling pathways, was associated with impaired proliferation and persistence. Therefore, these findings suggest that not the inhibition of early T cell activation alone, but the transcriptional shift caused by low-dose MEKi affects the balance that governs T cell stemness, exhaustion, and persistence. In fact, a tilt in the balance of transcription factor activity towards dominance of NFAT over AP-1 was shown to induce exhaustion and vice versa.[64] Interestingly, the transcriptional shift on MEKi was paralleled by a shift in cytokine profile, marked by decreased levels of CD8+ effector cytokines, and by increased GNLY secretion. It was previously reported that the transactivation of the GNLY promoter dominantly depends on transcription factor AP-1, but not NFκB.[65]

In conclusion, our analysis highlights the importance of carefully tuning T cell activation levels in ACT, consistent with our previous findings.[11] Our results support combinatorial treatment strategies with transient, low-dose administration of MAPK-signaling inhibitors to decrease T cell stimulation strength of otherwise overstimulated engineered T cell products while enhancing their cytotoxic function and persistence. Therefore, harnessing a more moderate level of T cell activation emerges as a promising approach to improve the design of next-generation T cell-based immunotherapies in clinical settings.

Author affiliations
[1]School of Medicine and Health, III Medical Department, TUM University Hospital, Technical University of Munich, Munich, Germany
[2]Center for Translational Cancer Research (TranslaTUM), Technical University of Munich, Munich, Germany
[3]Institute of Medical Microbiology Immunology and Hygiene, Technical University of Munich, Munich, Germany
[4]Institute of Molecular Oncology and Functional Genomics, TUM School of Medicine and Health, Technical University of Munich, Munich, Germany
[5]German Center for Infection Research, Munich Site, Munich, Germany
[6]Bavarian Cancer Research Center, Erlangen, Germany
[7]German Cancer Consortium (DKTK), partner-site Munich, German Cancer Research Center (DKFZ), Heidelberg, Germany

Acknowledgements The authors thank patient Mel15 and all healthy donors for participating in the study and for their continuous support. The authors thank Professor Dr Peter Steinberger (University of Vienna, Austria) for providing the Jurkat triple parameter reporter system (JE6.1 TPR) and Professor Dr Tobias Feuchtinger

Journal for ImmunoTherapy of Cancer: first published as 10.1136/jitc-2025-012800 on 1 December 2025. Downloaded from https://jitc.bmj.com on 12 February 2026 by guest. Protected by copyright, including for uses related to text and data mining, AI training, and similar technologies.

(Universität Freiburg, Germany) for providing the aCD19-CAR constructs for all CAR-T analyses. The authors thank the Core Facility Comparative Experimental Pathology (Institute of Pathology, TUM, Munich) for performing IHC sample preparation and staining as well as the Core Facility Cell Analysis (TranslaTUM, Munich) for supporting flow cytometric readout. The authors used Grammarly and ChatGPT to improve grammar and phrasing for some parts of this manuscript. Both tools were used solely for language editing purposes. All content was reviewed, edited, and approved by the authors to ensure accuracy and integrity.

Contributors Conceptualization: FF. Methodology: FF, AS, MF, LR, GZ, PAdM, EC, SB, RÖ, DHB, FB, AMK. Experimental work: FF, AS, MF, LR, GZ, PAdM, EC, SB, RÖ. Data analysis: FF, AS, MF. Visualization: FF, AS, MF. Funding acquisition: DHB, FB, AMK. Project administration: FF, AMK. Supervision: AMK. Writing—original draft: FF. Writing—review and editing: all authors. FF is the guarantor of this work and accepts full responsibility for the integrity of the data and the accuracy of the analysis.

Funding This project was supported by the European Institute of Innovation and Technology (EIT) Health 19638 (AMK); the Deutsche Forschungsgemeinschaft (DFG, German Research Foundation)—SFB824 (C10 AMK); SFB-TRR 338/1 2021—452881907 (A03 AMK/A01 DHB); SFB-TRR 387/1—514894665 (FB); and BA 2851/7-1, project ID: 537477296 (FB). PAdM is supported by the Swiss National Science Foundation (P500PB_222048) and has received funding from the European Union's Horizon 2020 Research and Innovation Program under the Marie Skłodowska-Curie grant agreement no. 101152312.

Competing interests No, there are no competing interests.

Patient consent for publication Not applicable.

Ethics approval This research and all experiments align with the regulations and approval of the institutional review board (Ethics Commission, Faculty of Medicine, project nr. 5722/13, 193/17S, and 521/18S) of Technical University of Munich and are in accordance with principles put forth in the Declaration of Helsinki. Informed consent of all participants in this study was granted in written form.

Provenance and peer review Not commissioned; externally peer reviewed.

Data availability statement Data are available on reasonable request. All data relevant to the study are included in the article or uploaded as supplementary information. All data and code are available upon reasonable request. All data relevant to the study are included in the article or uploaded as supplementary information.

Supplemental material This content has been supplied by the author(s). It has not been vetted by BMJ Publishing Group Limited (BMJ) and may not have been peer-reviewed. Any opinions or recommendations discussed are solely those of the author(s) and are not endorsed by BMJ. BMJ disclaims all liability and responsibility arising from any reliance placed on the content. Where the content includes any translated material, BMJ does not warrant the accuracy and reliability of the translations (including but not limited to local regulations, clinical guidelines, terminology, drug names and drug dosages), and is not responsible for any error and/or omissions arising from translation and adaptation or otherwise.

Open access This is an open access article distributed in accordance with the Creative Commons Attribution Non Commercial (CC BY-NC 4.0) license, which permits others to distribute, remix, adapt, build upon this work non-commercially, and license their derivative works on different terms, provided the original work is properly cited, appropriate credit is given, any changes made indicated, and the use is non-commercial. See https://creativecommons.org/licenses/by-nc/4.0/.

ORCID iDs
Franziska Füchsl https://orcid.org/0000-0001-5069-1442
Gabriela Zuleger https://orcid.org/0009-0003-6771-3005
Priska Auf der Maur https://orcid.org/0000-0002-9059-8979
Sarah Braun https://orcid.org/0009-0009-9244-1033
Angela M Krackhardt https://orcid.org/0000-0002-4752-0543

REFERENCES

1 Cappell KM, Kochenderfer JN. Long-term outcomes following CAR T cell therapy: what we know so far. *Nat Rev Clin Oncol* 2023;20:359–71.
2 D'Angelo SP, Araujo DM, Abdul Razak AR, *et al*. Afamitresgene autoleucel for advanced synovial sarcoma and myxoid round cell liposarcoma (SPEARHEAD-1): an international, open-label, phase 2 trial. *Lancet* 2024;403:1460–71.
3 Schoenfeld AJ, Lee SM, Doger de Spéville B, *et al*. Lifileucel, an Autologous Tumor-Infiltrating Lymphocyte Monotherapy, in Patients with Advanced Non-Small Cell Lung Cancer Resistant to Immune Checkpoint Inhibitors. *Cancer Discov* 2024;14:1389–402.
4 Foy SP, Jacoby K, Bota DA, *et al*. Non-viral precision T cell receptor replacement for personalized cell therapy. *Nature New Biol* 2023;615:687–96.
5 Parkhurst M, Goff SL, Lowery FJ, *et al*. Adoptive transfer of personalized neoantigen-reactive TCR-transduced T cells in metastatic colorectal cancer: phase 2 trial interim results. *Nat Med* 2024;30:2586–95.
6 Borgers JSW, Lenkala D, Kohler V, *et al*. Personalized, autologous neoantigen-specific T cell therapy in metastatic melanoma: a phase 1 trial. *Nat Med* 2025;31:881–93.
7 de Witte MA, Coccoris M, Wolkers MC, *et al*. Targeting self-antigens through allogeneic TCR gene transfer. *Blood* 2006;108:870–7.
8 Purcarea A, Jarosch S, Barton J, *et al*. Signatures of recent activation identify a circulating T cell compartment containing tumor-specific antigen receptors with high avidity. *Sci Immunol* 2022;7:eabm2077.
9 Bassani-Sternberg M, Bräunlein E, Klar R, *et al*. Direct identification of clinically relevant neoepitopes presented on native human melanoma tissue by mass spectrometry. *Nat Commun* 2016;7:13404.
10 Bräunlein E, Lupoli G, Füchsl F, *et al*. Functional analysis of peripheral and intratumoral neoantigen-specific TCRs identified in a patient with melanoma. *J Immunother Cancer* 2021;9:e002754.
11 Füchsl F, Untch J, Kavaka V, *et al*. High-resolution profile of neoantigen-specific TCR activation links moderate stimulation to increased resilience of engineered TCR-T cells. *Nat Commun* 2024;15:10520.
12 Straub A, Grassmann S, Jarosch S, *et al*. Recruitment of epitope-specific T cell clones with a low-avidity threshold supports efficacy against mutational escape upon re-infection. *Immunity* 2023;56:1269–84.
13 Robbins PF, Li YF, El-Gamil M, *et al*. Single and dual amino acid substitutions in TCR CDRs can enhance antigen-specific T cell functions. *J Immunol* 2008;180:6116–31.
14 Stadtmauer EA, Faitg TH, Lowther DE, *et al*. Long-term safety and activity of NY-ESO-1 SPEAR T cells after autologous stem cell transplant for myeloma. *Blood Adv* 2019;3:2022–34.
15 Poncette L, Chen X, Lorenz FK, *et al*. Effective NY-ESO-1-specific MHC II-restricted T cell receptors from antigen-negative hosts enhance tumor regression. *J Clin Invest* 2019;129:120391:324–35:.
16 Singhaviranon S, Dempsey JP, Hagymasi AT, *et al*. Low-avidity T cells drive endogenous tumor immunity in mice and humans. *Nat Immunol* 2025;26:240–51.
17 Shakiba M, Zumbo P, Espinosa-Carrasco G, *et al*. TCR signal strength defines distinct mechanisms of T cell dysfunction and cancer evasion. *J Exp Med* 2022;219:e20201966.
18 Klebanoff CA, Crompton JG, Leonardi AJ, *et al*. Inhibition of AKT signaling uncouples T cell differentiation from expansion for receptor-engineered adoptive immunotherapy. *JCI Insight* 2017;2:e95103.
19 Zheng W, O'Hear CE, Alli R, *et al*. PI3K orchestration of the in vivo persistence of chimeric antigen receptor-modified T cells. *Leukemia* 2018;32:1157–67.
20 Weber EW, Parker KR, Sotillo E, *et al*. Transient rest restores functionality in exhausted CAR-T cells through epigenetic remodeling. *Science* 2021;372:eaba1786.
21 Mestermann K, Giavridis T, Weber J, *et al*. The tyrosine kinase inhibitor dasatinib acts as a pharmacologic on/off switch for CAR T cells. *Sci Transl Med* 2019;11:eaau5907.
22 Zhang H, Hu Y, Shao M, *et al*. Dasatinib enhances anti-leukemia efficacy of chimeric antigen receptor T cells by inhibiting cell differentiation and exhaustion. *J Hematol Oncol* 2021;14:113.
23 Lombardo LJ, Lee FY, Chen P, *et al*. Discovery of N-(2-chloro-6-methyl- phenyl)-2-(6-(4-(2-hydroxyethyl)- piperazin-1-yl)-2-methylpyrimidin-4- ylamino)thiazole-5-carboxamide (BMS-354825), a dual Src/Abl kinase inhibitor with potent antitumor activity in preclinical assays. *J Med Chem* 2004;47:6658–61.
24 Ascierto PA, McArthur GA, Dréno B, *et al*. Cobimetinib combined with vemurafenib in advanced BRAF(V600)-mutant melanoma (coBRIM): updated efficacy results from a randomised, double-blind, phase 3 trial. *Lancet Oncol* 2016;17:1248–60.
25 Rice KD, Aay N, Anand NK, *et al*. Novel Carboxamide-Based Allosteric MEK Inhibitors: Discovery and Optimization Efforts toward XL518 (GDC-0973). *ACS Med Chem Lett* 2012;3:416–21.
26 Ebert PJR, Cheung J, Yang Y, *et al*. MAP Kinase Inhibition Promotes T Cell and Anti-tumor Activity in Combination with PD-L1 Checkpoint Blockade. *Immunity* 2016;44:609–21.
27 Verma V, Jafarzadeh N, Boi S, *et al*. MEK inhibition reprograms $CD8^+$ T lymphocytes into memory stem cells with potent antitumor effects. *Nat Immunol* 2021;22:53–66.

Journal for ImmunoTherapy of Cancer: first published as 10.1136/jitc-2025-012800 on 1 December 2025. Downloaded from https://jitc.bmj.com on 12 February 2026 by guest. Protected by copyright, including for uses related to text and data mining, AI training, and similar technologies.

28 Hellmann MD, Kim T-W, Lee CB, *et al*. Phase Ib study of atezolizumab combined with cobimetinib in patients with solid tumors. *Ann Oncol* 2019;30:1134–42.
29 Gogas H, Dréno B, Larkin J, *et al*. Cobimetinib plus atezolizumab in BRAF^{V600} wild-type melanoma: primary results from the randomized phase III IMspire170 study. *Ann Oncol* 2021;32:384–94.
30 Hieken TJ, Nelson GD, Flotte TJ, *et al*. Neoadjuvant cobimetinib and atezolizumab with or without vemurafenib for high-risk operable Stage III melanoma: the Phase II NeoACTIVATE trial. *Nat Commun* 2024;15:1430.
31 Wang X, Tao X, Chen P, *et al*. MEK inhibition prevents CAR-T cell exhaustion and differentiation via downregulation of c-Fos and JunB. *Sig Transduct Target Ther* 2024;9:293.
32 Stenger D, Stief TA, Kaeuferle T, *et al*. Endogenous TCR promotes in vivo persistence of CD19-CAR-T cells compared to a CRISPR/Cas9-mediated TCR knockout CAR. *Blood* 2020;136:1407–18.
33 Schober K, Müller TR, Gökmen F, *et al*. Orthotopic replacement of T-cell receptor α- and β-chains with preservation of near-physiological T-cell function. *Nat Biomed Eng* 2019;3:974–84.
34 Müller TR, Jarosch S, Hammel M, *et al*. Targeted T cell receptor gene editing provides predictable T cell product function for immunotherapy. *Cell Rep Med* 2021;2:100374.
35 Klar R, Schober S, Rami M, *et al*. Therapeutic targeting of naturally presented myeloperoxidase-derived HLA peptide ligands on myeloid leukemia cells by TCR-transgenic T cells. *Leukemia* 2014;28:2355–66.
36 Jutz S, Leitner J, Schmetterer K, *et al*. Assessment of costimulation and coinhibition in a triple parameter T cell reporter line: Simultaneous measurement of NF-κB, NFAT and AP-1. *J Immunol Methods* 2016;430:10–20.
37 Müller TR, Schuler C, Hammel M, *et al*. A T-cell reporter platform for high-throughput and reliable investigation of TCR function and biology. *Clin Transl Immunology* 2020;9:e1216.
38 Parekh S, Ziegenhain C, Vieth B, *et al*. The impact of amplification on differential expression analyses by RNA-seq. *Sci Rep* 2016;6:25533.
39 Love MI, Huber W, Anders S. Moderated estimation of fold change and dispersion for RNA-seq data with DESeq2. *Genome Biol* 2014;15:550.
40 Wilhelm M, Zolg DP, Graber M, *et al*. Deep learning boosts sensitivity of mass spectrometry-based immunopeptidomics. *Nat Commun* 2021;12:3346.
41 Choi BD, Yu X, Castano AP, *et al*. CAR-T cells secreting BiTEs circumvent antigen escape without detectable toxicity. *Nat Biotechnol* 2019;37:1049–58.
42 Lim SY, Lin Y, Lee JH, *et al*. Single-cell RNA sequencing reveals melanoma cell state-dependent heterogeneity of response to MAPK inhibitors. *EBioMedicine* 2024;107:105308.
43 Pratilas CA, Taylor BS, Ye Q, *et al*. (V600E)BRAF is associated with disabled feedback inhibition of RAF-MEK signaling and elevated transcriptional output of the pathway. *Proc Natl Acad Sci U S A* 2009;106:4519–24.
44 Daniel B, Yost KE, Hsiung S, *et al*. Divergent clonal differentiation trajectories of T cell exhaustion. *Nat Immunol* 2022;23:1614–27.
45 Sugiyarto G, Lau D, Hill SL, *et al*. Reactivation of low avidity tumor-specific CD8^{+} T cells associates with immunotherapeutic efficacy of anti-PD-1. *J Immunother Cancer* 2023;11:e007114.
46 Presotto D, Erdes E, Duong MN, *et al*. Fine-Tuning of Optimal TCR Signaling in Tumor-Redirected CD8 T Cells by Distinct TCR Affinity-Mediated Mechanisms. *Front Immunol* 2017;8:1564.
47 Schmid DA, Irving MB, Posevitz V, *et al*. Evidence for a TCR affinity threshold delimiting maximal CD8 T cell function. *J Immunol* 2010;184:4936–46.
48 Slansky JE, Jordan KR. The Goldilocks model for TCR-too much attraction might not be best for vaccine design. *PLoS Biol* 2010;8:e1000482.
49 Hu-Lieskovan S, Mok S, Homet Moreno B, *et al*. Improved antitumor activity of immunotherapy with BRAF and MEK inhibitors in BRAF(V600E) melanoma. *Sci Transl Med* 2015;7:279ra41.
50 Liu L, Mayes PA, Eastman S, *et al*. The BRAF and MEK Inhibitors Dabrafenib and Trametinib: Effects on Immune Function and in Combination with Immunomodulatory Antibodies Targeting PD-1, PD-L1, and CTLA-4. *Clin Cancer Res* 2015;21:1639–51.
51 Choi H, Deng J, Li S, *et al*. Pulsatile MEK Inhibition Improves Anti-tumor Immunity and T Cell Function in Murine Kras Mutant Lung Cancer. *Cell Rep* 2019;27:806–19.
52 Dennison L, Ruggieri A, Mohan A, *et al*. Context-Dependent Immunomodulatory Effects of MEK Inhibition Are Enhanced with T-cell Agonist Therapy. *Cancer Immunol Res* 2021;9:1187–201.
53 Rosen LS, LoRusso P, Ma WW, *et al*. A first-in-human phase I study to evaluate the MEK1/2 inhibitor, cobimetinib, administered daily in patients with advanced solid tumors. *Invest New Drugs* 2016;34:604–13.
54 Badovinac VP, Messingham KAN, Jabbari A, *et al*. Accelerated CD8+ T-cell memory and prime-boost response after dendritic-cell vaccination. *Nat Med* 2005;11:748–56.
55 Haring JS, Badovinac VP, Harty JT. Inflaming the CD8. *Immunity* 2006;25:19–29.
56 Ratner A, Clark WR. Role of TNF-alpha in CD8+ cytotoxic T lymphocyte-mediated lysis. *J Immunol* 1993;150:4303–14.
57 Ding X, Yang W, Shi X, *et al*. TNF Receptor 1 Mediates Dendritic Cell Maturation and CD8 T Cell Response through Two Distinct Mechanisms. *The Journal of Immunology* 2011;187:1184–91.
58 Zheng L, Fisher G, Miller RE, *et al*. Induction of apoptosis in mature T cells by tumour necrosis factor. *Nature New Biol* 1995;377:348–51.
59 Bertrand F, Montfort A, Marcheteau E, *et al*. TNFα blockade overcomes resistance to anti-PD-1 in experimental melanoma. *Nat Commun* 2017;8:2256.
60 Falvo JV, Tsytsykova AV, Goldfeld AE. Transcriptional control of the TNF gene. *Curr Dir Autoimmun* 2010;11:27–60.
61 Vanden Berghe W, Plaisance S, Boone E, *et al*. p38 and Extracellular Signal-regulated Kinase Mitogen-activated Protein Kinase Pathways Are Required for Nuclear Factor-κB p65 Transactivation Mediated by Tumor Necrosis Factor. *Journal of Biological Chemistry* 1998;273:3285–90.
62 Saha RN, Jana M, Pahan K. MAPK p38 Regulates Transcriptional Activity of NF-κB in Primary Human Astrocytes via Acetylation of p65. *J Immunol* 2007;179:7101–9.
63 Madrid LV, Mayo MW, Reuther JY, *et al*. Akt Stimulates the Transactivation Potential of the RelA/p65 Subunit of NF-κB through Utilization of the IκB Kinase and Activation of the Mitogen-activated Protein Kinase p38. *Journal of Biological Chemistry* 2001;276:18934–40.
64 Martinez GJ, Pereira RM, Äijö T, *et al*. The Transcription Factor NFAT Promotes Exhaustion of Activated CD8 + T Cells. *Immunity* 2015;42:265–78.
65 Kida Y, Shimizu T, Kuwano K. Opposing roles of activator protein-1 and CCAAT/enhancer binding protein β in the regulation of inducible granulysin gene expression in a human monocytic cell line, THP-1. *Immunology* 2002;107:507–16.

Journal for ImmunoTherapy of Cancer: first published as 10.1136/jitc-2025-012800 on 1 December 2025. Downloaded from https://jitc.bmj.com on 12 February 2026 by guest. Protected by copyright, including for uses related to text and data mining, AI training, and similar technologies.